A&A 491, L37–L40 (2008)
DOI: 10.1051/0004-6361:200810505


Astronomy & Astrophysics

Letter to the Editor

# On the rapid TeV flaring activity of Markarian 501

A. Mastichiadis and K. Moraitis

Department of Physics, University of Athens, Panepistimiopolis, GR 15783 Zografos, Greece
e-mail: amastich@phys.uoa.gr

Received 2 July 2008 / Accepted 11 October 2008

**ABSTRACT**

*Aims.* We investigate the one-zone SSC model of TeV blazars in the presence of electron acceleration. In this picture, electrons achieve their maximum energy as the acceleration saturates due to a combination of synchrotron and inverse Compton scattering losses.
*Methods.* We solve the spatially averaged kinetic equations that describe the simultaneous evolution of particles and photons, obtaining the multiwavelength spectrum as a function of time.
*Results.* We apply the model to the rapid flare of Mrk 501 of July 9, 2005 as observed by the MAGIC telescope, and derive the relevant parameters for the pre-flare quasi-steady-state and the states during the flare. We demonstrate that a hard lag flare can be obtained with parameters well inside the range expected for this source. In particular, a high value of Doppler factor appears necessary.

**Key words.** galaxies: BL Lacertae objects: individual: Mrk 501 – galaxies: jets – gamma rays: theory – X-rays: galaxies – acceleration of particles – radiation mechanisms: non-thermal

## 1. Introduction

Blazars, a class of Active Galactic Nuclei, have multiwavelength spectra with two distinct components: the first, which is generally believed to be produced by electron synchrotron radiation, reaches a maximum depending on the object, between the optical and X-ray regime; the second, which is probably produced by inverse Compton scattering of the same relativistic electrons either on the synchrotron photons (Maraschi et al. 1992) or on some other photon population, external to the source (Dermer et al. 1992; Sikora et al. 1994), reaches its maximum in the GeV to TeV $\gamma$-ray band. This emission is assumed to be produced within a relativistic flow directed towards us and therefore to be Doppler boosted.

Flaring activity is probably the most distinctive characteristic of these objects. This is true in particular for the X-ray and TeV regimes, which are produced by radiation from electrons of close to their maximum energy. In the X-ray regime, flares have therefore been observed on timescales of hours to days (Kataoka et al. 2001), while in the TeV regime the variability can be even faster (Gaidos et al. 1996; Albert et al. 2007; Aharonian et al. 2007).

Mrk 501 was reported to show an episode of flaring activity in the TeV regime where hard $\gamma$-rays lagged soft by approximately four minutes. This flare manifested a combination of rapid variability and spectral evolution. Flares showing a hard lag have been observed before in the X-ray regime (see, for example, Brinkmann et al. 2005; Sato et al. 2008), in addition to flares showing a soft lag (Takahashi et al. 1996). However, it has not been possible to obtain this detailed spectral information in the $\gamma$-rays.

In general, soft lags can be interpreted as being due to electron cooling. If electrons are either accelerated rapidly to their maximum energy or injected as secondaries, then, since the more energetic electrons cool more rapidly, they will produce first a variation in hard photons followed by a variation in softer ones, exhibiting therefore a soft lag (Kirk et al. 1998, hereafter KRM; Kirk & Mastichiadis 1999; Kusunose et al. 2000).

An explanation of hard lags requires some type of particle acceleration (for a different explanation, see Albert et al. 2008). If the timescale associated with acceleration is shorter than the timescale for particle cooling, then the radiation emitted from particles accelerating from low to high energies will show a hard lag. However, since the electrons accelerated to high energies have insufficient time to cool before reaching their maximum energy, the amount of radiation produced is small and the mechanism is therefore inefficient. Hard lags will therefore be more evident close to the spectral cutoff, where, by definition, the radiative loss timescale is comparable with that of acceleration (KRM).

In the present paper, we examine the unique properties of the July 2005 flare of Mrk 501 within the context of the one-zone SSC model, which has been modified to include electron acceleration. Our goal is to determine whether the model can provide reasonable fitting parameters for both the steady state and the flaring activity. In Sect. 2, we outline the model, in Sect. 3 we describe the procedure of reproducing both the quasi steady state and the flare and, we present our conclusions in Sect. 4.

## 2. The model

To model the emission of Mrk 501, we use a similar approach to Mastichiadis & Kirk (1997, hereafter MK97), i.e. we solve simultaneously two time-dependent kinetic equations for the distribution functions of electrons and photons. The electron equation is given by

$$\frac{\partial n_e}{\partial t} + \frac{\partial}{\partial \gamma}\left(\frac{\gamma}{t_{acc}} n_e\right) + \frac{n_e}{t_{esc}} + \mathcal{L}^{syn} + \mathcal{L}^{ics} = Q(t)\delta(\gamma - \gamma_0) + Q^{\gamma\gamma}, \quad (1)$$

while the photon equation is

$$\frac{\partial n_\gamma}{\partial t} + \frac{n_\gamma}{t_{cr}} + \mathcal{L}^{\gamma\gamma} + \mathcal{L}^{ssa} = Q^{syn} + Q^{ics}. \quad (2)$$

The operators $\mathcal{L}$ denote losses and escape from the system, while $Q$ denote injection and source terms. The unknown functions $n_e$ are $n_\gamma$ are the differential number densities of electrons and photons, respectively, and the physical processes included in the kinetic equations are: (1) electron synchrotron radiation and synchrotron self absorption (denoted by the superscripts "syn"and "ssa"respectively); (2) inverse Compton scattering (both in the Thomson and Klein-Nishina regimes) ("ics"); and (3) photon-photon pair production ("$\gamma\gamma$").

The physical processes listed above are modeled in a way as described in Mastichiadis & Kirk (1995, hereafter MK95), where a detailed description of the functional form of the above operators is given. The current version of the code also includes some improvements over MK95. In the case of synchrotron radiation, relativistic electrons therefore emit the full photon spectrum (see e.g. Blumenthal & Gould 1970), instead of the delta-function approximation used in MK95. For inverse Compton scattering, while the electron cooling still uses the technique described by MK95, the photon emissivity is modeled using Eq. (2.48) of Blumenthal & Gould (1970). Numerical tests have shown that this approach balances electron energy losses and total photon radiated power to within 90% of each other.

Furthermore, departing from the approach of MK97, we implement an acceleration term in the electron kinetic equation, which is characterized by an appropriate timescale ($t_{acc}$) and accompanied by a term describing particle injection at some low energy (first term in RHS of Eq. (1), where $Q(t)$ is the rate of electrons injected at low energies $\gamma_0 m_e c^2$). This modification allows us to follow particles as they accelerate from low to high energies. We note that this approach is similar to that taken by KRM. However, the present work differs from KRM in that we adopt a one-zone model.

There are six parameters required to specify the source in a stationary state. These include

1. the Doppler factor $\delta = [\Gamma(1 - \beta\cos\theta)]^{-1}$.
2. the radius $R$ of the source (or, equivalently, the crossing time in the rest frame of the source $t_{cr} = R/c$);
3. the magnetic field strength $B$;
4. the acceleration timescale $t_{acc}$, which in the setup of the problem must obey the condition $t_{acc} \geq t_{cr}$;
5. the timescale of particle escape of the system $t_{esc}$;
6. the rate of injected electrons $Q_0$ – we note, however, that the solution becomes largely independent of the exact choice of $\gamma_0$ as long as this is not higher than 10.

As shown by KRM this prescription (under the assumption of synchrotron radiation losses only) corresponds to an electron distribution function, which, in its steady state is expressed by

$$n_e(\gamma) \propto \gamma^{-2}\left(\frac{1}{\gamma} - \frac{1}{\gamma_{max}}\right)^{(t_{acc}-t_{esc})/t_{esc}} \quad (3)$$

for $\gamma_0 \leq \gamma \leq \gamma_{max}$, where $\gamma_{max}$ is the Lorentz factor at which electron energy losses balance acceleration. For example, in the pure synchrotron case,

$$\gamma_{max} = (\beta_s t_{acc})^{-1} \quad (4)$$

where $\beta_s = \frac{4}{3}\sigma_T c\frac{B^2}{8\pi m_e c^2}$ and $\sigma_T$ is the Thomson cross section. However, the present approach incorporates, in addition to synchrotron, SSC losses, which render the derivation of an analytic solution impossible due to complications arising from the Klein-Nishina limit. One further notes that when both $t_{acc}$ and $t_{esc}$ are independent of energy, as was assumed in deriving the above solution, the electron distribution function is a power law of index $s = -2 - (t_{acc} - t_{esc})/t_{esc}$ (as long as $\gamma \ll \gamma_{max}$). We also note that tests on the code in the pure synchrotron loss case have shown that the electron distribution above $\gamma_{max}$ does not decline to zero abruptly, but rather, due to numerical diffusion, a steep power law is produced.

The above description changes during a flare. We assume that the system has reached some stationary state. If this is perturbed in some way, i.e. by injecting an increased particle rate into the acceleration mechanism for some time interval $\Delta\tau$, then a wave of fresh particles will move to high energies. Assuming that the episode starts at some instant $t_0$, then at each time $t > t_0 + \Delta\tau$ the fresh particles will have Lorentz factors $\gamma_{fl,min}(t) \leq \gamma \leq \gamma_{fl,max}(t)$ with $\gamma_{fl,max}(t) = \gamma_0 e^{(t-t_0)/t_{acc}}$ and $\gamma_{fl,min}(t) = \gamma_0 e^{(t-t_0-\Delta\tau)/t_{acc}}$. This relation holds as long as $\gamma_{fl,max} \leq \gamma_{max}$. Since the time evolving particle distribution will be of larger amplitude than the steady state one, this will cause a flare in photons that will relax back to the pre-flare state as soon as particles of Lorentz factor $\gamma_{fl,min}$ begin to assume values approximately equal to $\gamma_{max}$. It is interesting to note that since the losses are mot entirely due to synchrotron radiation but also to SSC, the flaring event could have an impact on the determination of $\gamma_{max}$. More specifically, the presence of extra photons during a flare in the system will increase the total electron energy losses and, depending on the specific conditions, could cause $\gamma_{max}$ to decline.

## 3. The July 9 2005 flare

We used the model described in the previous section to reproduce the X/TeV data shown in Fig. 21 of Albert et al. (2007) (July 9, 2005, observations). We solved the set of stiff differential equations given by Eqs. (1) and (2) using numerical techniques described and tested by MK95. The parameters used for the steady state fit were $R = 1.5\times10^{14}$ cm, $\delta = 60$, $B = 0.5$ G, $t_{acc} = 3t_{cr}$, $t_{esc} = 4.17t_{cr}$, $\gamma_0 = 10^{0.05}$, and $Q = 5\times10^6$ cm$^{-3}$ s$^{-1}$ erg$^{-1}$. The cosmological parameters used are $H_0 = 70$ km s$^{-1}$ Mpc$^{-1}$, $\Omega_\Lambda = 0.7$, and $\Omega = 0.3$. The spectrum indicated by a solid line in Fig. 1. The resulting electron distribution function is a power-law of slope $s = -1.7$ up to an energy $\gamma_{max} = 2\times10^5$.

Perturbing the steady state $n$ a way similar to that described above, we found that a change in $Q(t)$ always produces a hard lag flare as observed. However, this method of simulating a flaring activity causes the flux in each energy band to increase approximately by the same amplitude (see Mastichiadis & Moraitis 2009). If, as the observations appear to suggest, the flare also becomes harder, i.e. more flux is emitted in the higher energy bands, then to reproduce the TeV light-curve data, we require, in addition, to decrease $t_{acc}$ and/or $B$ during the flaring episode. This can be explained by inspection of Eq. (4). A spectral hardening of the flare requires an increase in $\gamma_{max}$ during the episode, which can be achieved, in the context of the present model, only by reducing one, or both, of the aforementioned parameters.

Figures 2 and 3 depict the light-curves produced by such a flaring episode. The observed flare originates from an impulsive change in $Q$ by a factor of ~13 for $\Delta\tau = 1t_{cr}$ and a decrease in $t_{acc}$ and $B$ by a factor of 1.7 for $\Delta\tau = 30t_{cr}$, which is approximately equal to the duration of the flaring episode, i.e. to the time needed for the injected particles to reach $\gamma_{max}$. To ensure that the spectral slope remains unchanged (see Eq. (3)), we also varied $t_{esc}$ by the same factor. Figure 2 shows the light-curve at the lowest energy range (0.15–0.25 TeV) of the MAGIC telescope, while Fig. 3 shows the corresponding light-curve at the

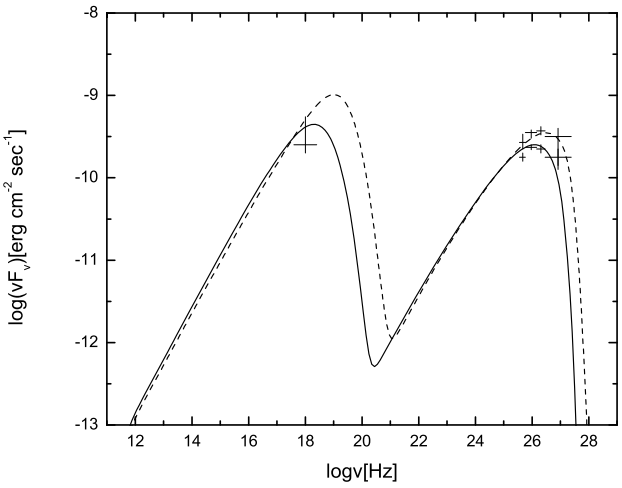


**Fig. 1.** Fit of the multi-wavelength spectrum of Mrk 501 during the flare discussed in the text. Solid curve is a fit to an assumed steady (or pre-flare) state as discussed by Albert et al. (2007). Parameters are as given in the text. The long dashed curve shows the spectrum at the instance where the fluence is maximum at the hard TeV band. The TeV spectra were de-absorbed as in Konopelko et al. (2003).

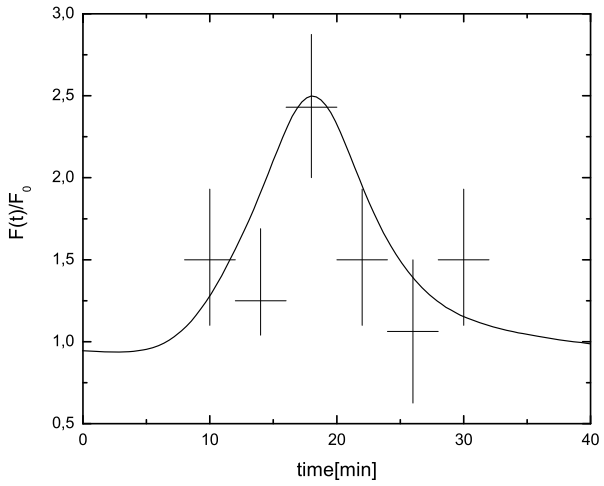


**Fig. 2.** Time evolution of the flare described in the text in the low (0.15–0.25 TeV) TeV band. Time is as measured by an observer in the lab frame. Observations were taken from Albert et al. (2007).

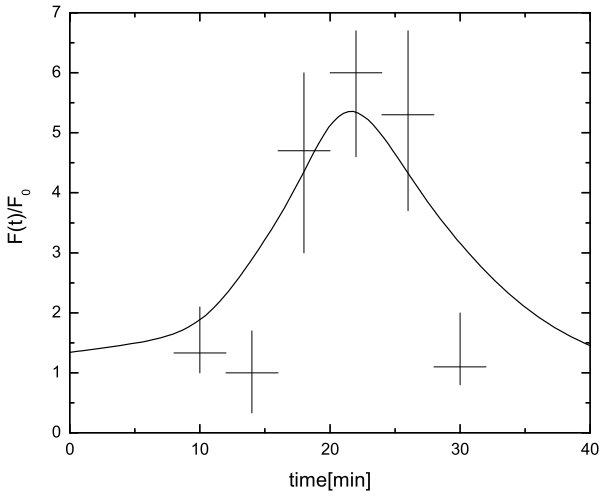


**Fig. 3.** Time evolution of the flare described in the text in the high (1.2–10 TeV) TeV band. Time is as measured by an observer in the lab frame. Observations were taken from Albert et al. (2007).

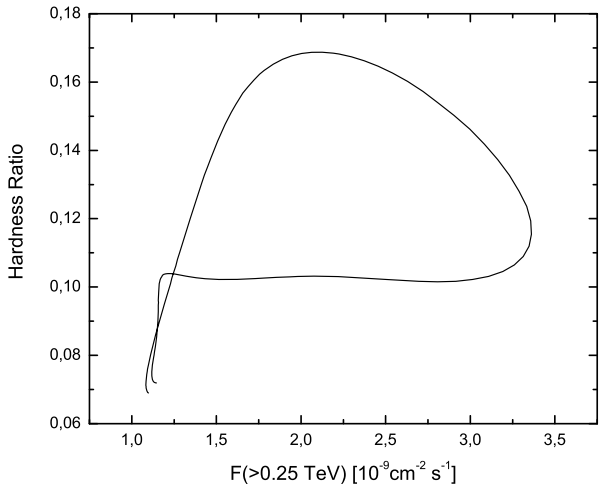


**Fig. 4.** Hardness ratio $F(1-10\ \mathrm{TeV})/F(0.25-1\ \mathrm{TeV})$ versus flux $F(>0.25\ \mathrm{TeV})$ for the flare described in the text. The curve rotates with time in an anticlockwise manner.

highest energy range (1.2–10 TeV). The time lag between the two energy bands is about three minutes.

The chosen flaring episode is too short to approach the stationary state corresponding to the new increased injection. Figure 1 shows, in addition to the pre-flare steady state, the multi-wavelength spectra at the instance at which the fluence reaches a maximum in the hard TeV band (long dashed line).

Figure 4 indicates the the derived TeV hardness ratio (defined to be $F(1-10\ \mathrm{TeV})/F(0.25-1\ \mathrm{TeV})$) versus the TeV flux, which, as expected, is anticlockwise.

## 4. Summary/Discussion

In the present paper, we have attempted to explain the rapid variability of Mrk 501 as observed by the MAGIC telescope in 2005 by using a one-zone model including particle acceleration and radiation. In this model, particles are injected into some acceleration mechanism at low energies and subsequently accelerated to high energies. They also radiate synchrotron and SSC radiation, which causes energy loss. The acceleration process saturates eventually at some particle energy when balanced by radiative losses. In this picture, the basic mechanism for producing hard lags as observed by MAGIC (Albert et al. 2007), could be a brief episode of enhanced particle injection. As the freshly injected particles reach high energies, they first radiate soft photons and then harder photons, creating a hard lag flare. This episode occurs on top of a quasi-steady-state that the particles were assumed to have achieved in the pre-flare state and to which they return in post-flare. According to this picture, MAGIC has therefore observed electron acceleration in action.

While hard lags can be explained by increasing the particle injection at low energies, the observed spectral hardening of the flare is reproduced only if, in addition, the acceleration timescale and/or the magnetic field strength are reduced over their pre-flare values. Even if variation in one of the above parameters can produce a spectral hardening, varying both simultaneously improves the light-curve fit. However, given the complexity of the overall flaring activity of TeV blazars, we consider the issue to be open, requiring more detailed observations.

The parameters used here are quite similar to those used by Konopelko et al. (2003). In both fits, we note the requirement for a high value of the Doppler factor. This is almost obligatory given the rapid variability of the flare (Begelman et al. 2008).

The presented model was an extension of the KRM model in the sense that it uses, in addition to synchrotron, SSC losses to balance acceleration. However, in contrast to KRM, it is a one-zone model, and it is therefore implicitly assumed that particles that escape do not radiate. This can be justified only if the magnetic field strength in the region where the particles escape is weaker than in the radiating zone. SSC losses also are expected to be lower outside the radiating zone because the synchrotron photon energy density decreases with distance (Gould 1979). Finally, we note that although the electron equation (Eq. (1)) is similar to one used in the kinetic description of diffusive shock acceleration (e.g. Ball & Kirk 1992), we have not specified a detailed method for particle acceleration. However, it is obvious that simultaneous variations in more than one parameter, as in the case here, need to be related to a specific theory of acceleration.

A prediction of this model is that a flare due to enhanced particle injection causes a hard lag behaviour also in the X-ray regime (Mastichiadis & Moraitis 2009). However, in non-steady situations, as is probably the case for flares, one expects to derive complicated relations between the synchrotron and the SSC component (see Katarzyński et al. 2005).

Bednarek & Wagner (2008) proposed another explanation for the hard lag by allowing the radiating blob to accelerate during the flare. In this case, the authors predicted that the delay between 20 and 200 GeV should be approximately one order of magnitude longer than the observed delay in the TeV band. On the other hand, our present model predicts that these rapidly varying flares should have the same time lag across the $\gamma$-ray band. Thus, coordinated future multiwavelength observations involving GLAST and Cherenkov detectors could help to determine whether the lag is due to acceleration of the blob itself or due to a brief episode of particle acceleration within a blob that moves with constant Lorentz factor $\Gamma$.

*Acknowledgements.* We would like to thank the referee for comments that helped improving the paper. This research was funded in part by a Grant from the Special Funds for Research (ELKE) of the University of Athens. K.M. acknowledges financial support from the Greek State Scholarships Foundation (IKY).

## References

Aharonian, F., Akhperjanian, A. G., Bazer-Bachi, A. R., et al. 2007, ApJ, 664, L71
Albert, J., Aliu, E., Anderhub, H., et al. 2007, ApJ, 669, 862
Albert, J., Aliu, E., Anderhub, H., et al. 2008, Phys. Lett. B, 668, 253
Ball, L., & Kirk, J. G. 1992, ApJ, 396, L39
Bednarek, W., & Wagner, R. M. 2008, A&A, 486, 679
Begelman, M. C., Fabian, A. C., & Rees, M. J. 2008, MNRAS, 384, L19
Blumenthal, G. R., & Gould, R. J. 1970, Rev. Mod. Phys., 42, 237
Brinkmann, W., Papadakis, I. E., Raeth, C., Mimica, P., & Haberl, F. 2005, A&A, 443, 397
Dermer, C. D., Schlickeiser, R., & Mastichiadis, A. 1992, A&A, 256, L27
Gaidos, J. A., Akerlof, C. W., Biller, S. D., et al. 1996, Nature, 383, 319
Gould, R. J. 1979, A&A, 76, 306
Kataoka, J., Takahashi, T., Wagner, S. J., et al. 2001, ApJ, 560, 659
Katarzyński, K., Ghisellini, G., Tavecchio, F., et al. 2005, A&A, 433, 479
Kirk, J. G., & Mastichiadis, A. 1999, Astropart. Phys., 11, 45
Kirk, J. G., Rieger, F. M., & Mastichiadis, A. 1998, A&A, 333, 452
Konopelko, A., Mastichiadis, A., Kirk, J., de Jager, O. C., & Stecker, F. W. 2003, ApJ, 597, 851
Kusunose, M., Takahara, F., & Li, H. 2000, ApJ, 536, 299
Maraschi, L., Ghisellini, G., & Celotti, A. 1992, ApJ, 397, L5
Mastichiadis, A., & Kirk, J. G. 1995, A&A, 295, 613
Mastichiadis, A., & Kirk, J. G. 1997, A&A, 320, 19
Mastichiadis, A., & Moraitis, K. 2009, Proc. of the Heidelberg Symp. (Gamma08)
Sato, R., Kataoka, J., Takahashi, T., et al. 2008, ApJ, 680, L9
Sikora, M., Begelman, M. C., & Rees, M. J. 1994, ApJ, 421, 153
Takahashi, T., Tashiro, M., Madejski, G., et al. 1996, ApJ, 470, L89